

Fluids of hard ellipsoids: Phase diagram including a nematic instability from Percus-Yevick theory

M. Letz and A. Latz

Johannes-Gutenberg Universität, 55099 Mainz, Germany

(Received 5 May 1999)

An important aspect of molecular fluids is the relation between orientation and translation parts of the two-particle correlations. Especially, a detailed knowledge of the influence of orientation correlations is needed to explain and calculate in detail the occurrence of a nematic phase. The simplest model system that shows both orientation and translation correlations is a system of hard ellipsoids. We investigate an isotropic fluid formed of hard ellipsoids with the Percus-Yevick theory. Solving the Percus-Yevick equations self-consistently and accurately in the high density regime gives, contrary to previous works, a clear criterion for a nematic instability. We calculate in detail the equilibrium phase diagram for a fluid of hard ellipsoids of revolution. Our results compare well with Monte Carlo simulations and density-functional theory. [S1063-651X(99)16311-6]

PACS number(s): 61.25.Em, 61.30.Cz, 61.20.Gy

I. INTRODUCTION

Isotropic simple liquids formed of atomic systems with rotational symmetry are well understood. If the two particle correlation is given by a hard sphere interaction an integral equation like the Percus-Yevick (PY) [1] closure relation can be solved analytically. For the liquid phase the PY equation gives good results even in the dense liquid regime (up to a packing fraction $\phi < 0.49$) above which the equilibrium state is crystalline, which PY fails to obtain. The packing fraction ϕ is defined as the relation between the number density ρ and the volume of the particles $\phi = (\pi/6)\rho\sigma^3$, with σ usually set to 1. For hard spheres, $\phi \approx 0.64$ corresponds to random closed packing and $\phi = \sqrt{2}\pi/6 \approx 0.74$ to packing in a fcc lattice.

Molecular systems have usually complicated potentials that are modeled, e.g., by Lennard-Jones potentials of each atom in a molecule. A very basic feature of molecular systems is the existence of orientation degrees of freedom that interplay in nontrivial ways with translational degrees of freedom. The simplest model system that allows us to study this interplay is a system of rotational symmetric hard ellipsoids. The equilibrium phase diagram is now—compared to hard spheres—enriched by an additional variable, the aspect ratio X_0 of the ellipsoids, which is defined as the ratio between the major axis a and the minor axis b , $X_0 = a/b$. Throughout the paper $b = 1$ is chosen. As a function of the aspect ratio or density a fluid of hard ellipsoids can now also undergo an isotropic to nematic (IN) transition. This is expected from the Onsager solution of hard spherocylinders [2], and has been found by computer simulations [3] and also by density-functional theory [4].

PY theory deals with the isotropic phase. It is not able to describe a phase transition. However, it is known from the hypernetted chain (HNC) closure relation for hard ellipsoids [5] and for dipolar hard spheres [6] that it is in principle possible to identify a precursor phenomenon of a phase transition in an integral equation. Such a precursor phenomenon is not known for the PY closure relation (see also [7]).

In this paper, however, we show that the PY closure re-

lation leads not only to a clear indication of a nematic instability but enables us also to calculate the equilibrium phase diagram of hard ellipsoids. Therefore we show that with respect to the description of a nematic instability PY theory is not inferior to the HNC.

II. INTEGRAL EQUATIONS

A fundamental relation that all closure relations for integral equations are based upon is the Ornstein-Zernike (OZ) equation [8]

$$h(\mathbf{r}_1, \Omega_1, \mathbf{r}_2, \Omega_2) = c(\mathbf{r}_1, \Omega_1, \mathbf{r}_2, \Omega_2) + \rho(c(\mathbf{r}_1, \Omega_1, \mathbf{r}_3, \Omega_3) \times h(\mathbf{r}_3, \Omega_3, \mathbf{r}_2, \Omega_2))_{\mathbf{r}_3, \Omega_3}. \quad (1)$$

It provides the relation between the total correlation function $h(\mathbf{r}_1, \Omega_1, \mathbf{r}_2, \Omega_2)$ and the direct correlation function $c(\mathbf{r}_1, \Omega_1, \mathbf{r}_2, \Omega_2)$. The product is given by

$$(\cdots)_{\mathbf{r}_3, \Omega_3} = \frac{1}{16\pi^2} \int d\Omega_3 \int d\mathbf{r}_3, \dots, \quad (2)$$

where \mathbf{r}_i is the position of the center of mass of the ellipsoid i and Ω_i is the orientation of this ellipsoid represented by the Euler angles Φ_i, θ_i (the third Euler angle χ is not needed due to the symmetry of the ellipsoids). Due to translational invariance the functions depend on $\mathbf{r}_{ij} = \mathbf{r}_i - \mathbf{r}_j$ only. In the following subsections we transform the OZ equations and the PY closure relation [Eq. (14)] in such a way that we can use it for a numerical treatment. With most of the definitions we follow the book of Gray and Gubbins [8].

A. Spherical harmonics

An obvious orthogonal basis set to expand the angular dependence of the correlation functions is given by spherical harmonics. The transformed correlation function $F \in \{c, h, \dots\}$ is given by

$$F(l_1, l_2, m; r) = i^{(l_1 - l_2)} \int d\Omega_1 \int d\Omega_2 F(\Omega_1, \Omega_2, r) \times Y_{l_1}^m(\Omega_1) Y_{l_2}^{m*}(\Omega_2). \quad (3)$$

Note that our transformation differs by a factor of $(-1)^m$ and by a factor of $i^{(l_1 - l_2)}$ from the definition used in the book of Gray and Gubbins [8]. The latter of these two factors gives us (in q frame) only real elements of the correlation functions. For Eq. (3) the r frame was used. This means the z axis of the coordinate system was chosen along the axis connecting the two particles that are correlated [8]. Therefore we only need to deal with one index m . In q space we use, after Fourier transformation, the laboratory fixed frame, the q frame [9,8], where now all q -dependent correlation functions are diagonal in m and m' . To be specific $\tilde{F}(l_1, l_2, m, m'; q) = \delta_{m, m'} \tilde{F}(l_1, l_2, m, m'; q) \equiv F(l_1, l_2, m; q)$. Within the complete set of spherical harmonics the OZ equation can be rewritten:

$$h(l_1, l_2, m; r) = c(l_1, l_2, m; r) + \frac{\rho}{4\pi} \sum_l \int dr_1 c(l_1, l, m; r_1) \times h(l, l_2, m; r - r_1). \quad (4)$$

This equation relates the total correlation function $h(l_1, l_2, m; r)$ with the direct correlation function $c(l_1, l_2, m; r)$. The total correlation function has two contributions, a direct one that results from direct correlations and is just $c(l_1, l_2, m; r)$ plus an indirect contribution that averages over possible interactions mediated by another particle in an indirect way.

B. Transformation into q space

Due to the expansion in spherical harmonics a Fourier transform cannot be performed as usual. First one has to find a representation of F that is invariant with respect to rotation:

$$F(l_1, l_2, l; r) = \sum_m \sqrt{\frac{4\pi}{(2l+1)}} F(l_1, l_2, m; r) \times C(l_1, l_2, l; m, -m, 0), \quad (5)$$

where $C(l_1, l_2, l; m_1, m_2, m)$ are the Clebsch-Gordan coefficients. The next step is the Hankel transformation, which uses the Rayleigh expansion to transform F from r space to q

space. This involves spherical Bessel functions $j_l(qr)$ due to the expansion of e^{iqr} within the basis of spherical harmonics:

$$F(l_1, l_2, l; q) = 4\pi(-i)^l \int_0^\infty j_l(qr) F(l_1, l_2, l; r). \quad (6)$$

In the final step one goes from the rotational invariant representation to the q frame and one gets a representation of F :

$$F(l_1, l_2, m; q) = \sum_l \sqrt{\frac{(2l+1)}{4\pi}} F(l_1, l_2, l; q) \times C(l_1, l_2, l; m, -m, 0). \quad (7)$$

Therefore Eqs. (5)–(7) transform a two particle correlation function given in real space and r frame into a function in q space and q frame.

C. The Ornstein-Zernike equations in q space

Applying Eqs. (5)–(7) to the OZ equation, one can rewrite Eq. (4):

$$h(l_1, l_2, m; q) = c(l_1, l_2, m; q) + \frac{\rho}{4\pi} \sum_l c(l_1, l, m; q) \times h(l, l_2, m; q). \quad (8)$$

This can be written as a matrix equation for each m and q value:

$$\underline{h}(m; q) = \underline{c}(m; q) + \frac{\rho}{4\pi} \underline{c}(m; q) \underline{h}(m; q), \quad (9)$$

where $\underline{c}, \underline{h}$ are symmetric matrices with indices l_1, l_2 .

For the input into our numerical calculation we define an auxiliary correlation function y in the usual way [8]:

$$\underline{y}(m; q) = \underline{h}(m; q) - \underline{c}(m; q). \quad (10)$$

Using this auxiliary function, the OZ equation is rewritten as

$$\left(1 - \frac{\rho}{4\pi} \underline{c}(m; q)\right) \underline{y}(m; q) = \frac{\rho}{4\pi} [\underline{c}(m; q)]^2. \quad (11)$$

This is a linear system of equations that determines $y(l_1, l_2, m; q)$ if $c(l_1, l_2, m; q)$ is known.

III. PERCUS-YEVICK CLOSURE RELATION

In a formal way one can define a product between two correlation functions $c = a * b$ [10]. In the r frame this product reads;

$$c(l_1, l_2, m; r) = \frac{1}{4\pi} \sum_{\substack{l'_1 l'_2 \\ l''_1 l''_2}} \sqrt{\frac{(2l'_1+1)(2l'_2+1)(2l''_1+1)(2l''_2+1)}{(2l_1+1)(2l_2+1)}} C(l'_1, l'_1, l_1; 0, 0, 0) C(l'_2, l'_2, l_2; 0, 0, 0) i^{l'_1 - l'_2 + l''_2 - l''_1} \times \sum_{m', m''} C(l'_1, l'_1, l_1; m', m'', m) C(l'_2, l'_2, l_2; -m', -m'', -m) a(l'_1, l'_2, m'; r) b(l''_1, l''_2, m''; r). \quad (12)$$

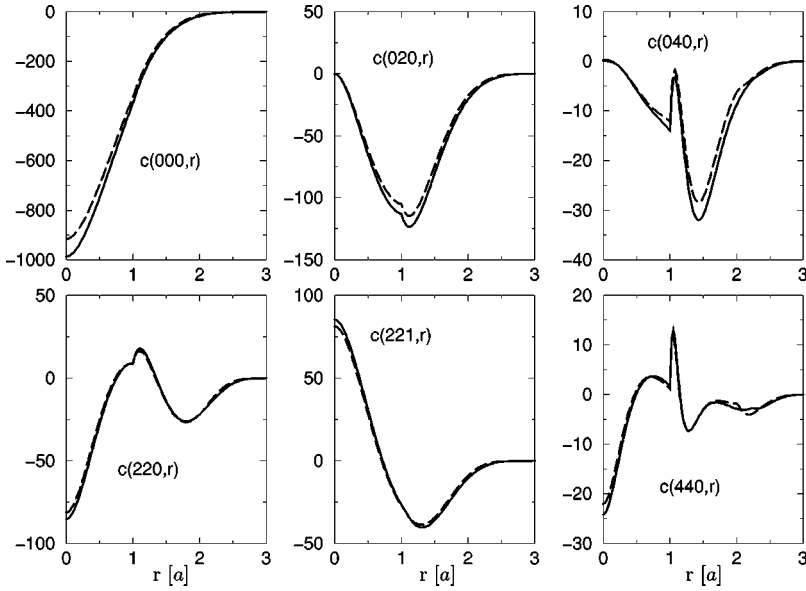


FIG. 1. For $X_0=3.0$ and $\phi=0.49$ already close to the nematic instability matrix elements of the direct correlation function $c(l_1, l_2, m, r)$ are compared. The curves with dashed lines are obtained with the exact ellipsoid overlap criterion, while the curves with solid lines show the results obtained with the Gaussian overlap model.

The Clebsch-Gordan coefficients enter into the equation due to spatial rotations that have to be performed.

The PY closure relation can now be expressed as

$$c = b * g, \quad (13)$$

where g is the pair correlation function and via $b = 1 - e^{\beta u}$ the pair potential u enters into the equation. For the purpose of solving the PY equation numerically it is better to rewrite Eq. (13) as a function of the auxiliary function y :

$$c = f * (y + 1), \quad (14)$$

where f is the Mayer function

$$f(\Omega_1, \Omega_2, r) = e^{-\beta u(\Omega_1, \Omega_2, r)} - 1. \quad (15)$$

The matrix elements of f in the basis set of spherical harmonics have to be computed using Eq. (3). This equation (14) determines the direct correlation function c if the auxiliary function y and the Mayer function f are known.

A. The pair potential

In order to determine the matrix elements of the Mayer function

$$f(\Omega_1, \Omega_2, r) = \begin{cases} 0 & \text{for } D(\Omega_1, \Omega_2, r) < r, \\ -1 & \text{for } D(\Omega_1, \Omega_2, r) \geq r, \end{cases} \quad (16)$$

we use the well known approximation of Berne and Pechukas [11], where D depends on the relative orientation of the two ellipsoids:

$$D(\Omega_1, \Omega_2, r) = \left[1 - \frac{1}{2} \chi \left(\frac{(\cos \theta_1 + \cos \theta_2)^2}{1 + \chi(\mathbf{e}_1 \mathbf{e}_2)} + \frac{(\cos \theta_1 - \cos \theta_2)^2}{1 - \chi(\mathbf{e}_1 \mathbf{e}_2)} \right) \right]^{-1/2}, \quad (17)$$

where \mathbf{e}_i are unit vectors along the symmetry axis of an ellipsoid on position i . This approximation models the interaction between two ellipsoids by the overlap of Gaussians. The value of χ is related to the aspect ratio of the ellipsoids

$$\chi = \frac{X_0^2 - 1}{X_0^2 + 1}. \quad (18)$$

Note that $D(\Omega_1, \Omega_2, r)$ is *not* invariant under $X_0 \rightarrow X_0^{-1}$, which implies $\chi \rightarrow -\chi$. To demonstrate the validity of the Gaussian overlap model we have plotted in Fig. 1 several matrix elements of the direct correlation function $c(l_1, l_2, m; r)$ for $X_0=3.0$ and $\phi=0.49$ (already close to the nematic instability). These are compared with results obtained with the exact ellipsoid overlap criterion. Compare also [12].

B. Symmetries of the solution

Due to the symmetries of the ellipsoid there are certain simplifications in the calculation that can be applied.

(i) Due to the head-tail symmetry of the ellipsoids all matrix elements of a correlation function $F(l_1, l_2, m, u) \in \{r, q\}$ with l_i odd are zero.

(ii) All elements of F are real both in r space and q space. Using the definition of Eq. (3) this is even valid for all linear molecules.

(iii) Therefore there is an additional symmetry $F(l_1, l_2, m, u) = F(l_1, l_2, -m, u)$.

(iv) Also the l occurring in the rotational invariants [Eq. (5)] can only have even values following from $l_1 + l_2 + l = \text{even}$, which results from inversion symmetry.

For a proof of (ii) and (iii) the reader may consult [13] and for (i) and (iv) one might look up [8]. There is one further feature we want to point out: For small argument (r or k), all nondiagonal elements ($l_1 \neq l_2$) have to vanish, at least in the isotropic phase:

$$\lim_{u \rightarrow 0} F(l_1, l_2, m; u) = 0 \quad \text{if } l_1 \neq l_2. \quad (19)$$

Using the definition $\tilde{F}(l_1, l_2, m, m; u) \equiv F(l_1, l_2, m, u)$, this follows from the transformation of \tilde{F} under rotations R :

$$\begin{aligned} & \lim_{u \rightarrow 0} \tilde{F}(l_1, l_2, m, m; Ru) \\ &= \lim_{u \rightarrow 0} \sum_{m_1, m_2} D_{m_1, m}^{l_1*}(R) D_{m_2, m}^{l_2}(R) \tilde{F}(l_1, l_2, m_1, m_2; u). \end{aligned} \quad (20)$$

This equation has to be valid for all R , which results in $\delta_{l_1, l_2} \delta_{m_1, m_2}$. This can be seen by integrating both sites of the above equation and by making use of the unitarity of the rotation matrices:

$$\begin{aligned} & \int dR \lim_{u \rightarrow 0} \tilde{F}(l_1, l_2, m, m; Ru) \\ &= 8\pi^2 \tilde{F}(l_1, l_2, m, m; 0) \\ &= \sum_{m_1, m_2} \int dR D_{m_1, m}^{l_1*}(R) D_{m_2, m}^{l_2}(R) \tilde{F}(l_1, l_2, m_1, m_2, 0) \\ &= \sum_{m_1, m_2} \frac{8\pi^2}{2l_1 + 1} \delta_{l_1, l_2} \delta_{m_1, m_2} \tilde{F}(l_1, l_2, m_1, m_2, 0). \end{aligned} \quad (21)$$

Therefore F has to vanish for small u for all nondiagonal elements ($l_1 \neq l_2$). This symmetry can clearly be seen from Fig. 2(c) and from Fig. 3(c). Further the value of the diagonal elements of $F(l_1, l_1, m, u \rightarrow 0)$ with $(2l_1 + 1)$ different m cannot (for short ranged potentials) depend on m .

C. Calculation procedure

In order to obtain a numerical solution of the equations above the following steps have to be performed:

(a) The matrix elements $f(l_1, l_2, m, r)$ of the Mayer function have to be computed using Eq. (3) and Eqs. (16)–(18). For our calculation we used 100 points in the range $\min(1, X_0) < r < \max(1, X_0)$, where r is given in units of the major axis a of the ellipsoids.

(b) An initial guess for $c(l_1, l_2, m, r)$ has to be made and a grid for r of $N_{max} = 400$ points in the range $0 < r < 10$ was chosen.

(c) The iteration begins by using Eqs. (5)–(7) to go from $c(l_1, l_2, m, r)$ in r space and r frame to $c(l_1, l_2, m, q)$ in q space and q frame using the Rayleigh transformation for the direct correlation function $c(l_1, l_2, m, r)$. It turned out to be crucial to use an analytic expansion of the spherical Bessel functions $j_l(x)$ for small argument x .

(d) The auxiliary function $y(l_1, l_2, m, q)$ has to be calculated using the OZ equations in the form of Eq. (11). As a q -space grid we used 400 points in the range $0 < q < 50$ where q is measured in units of $[2\pi/a]$.

(e) Using Eqs. (5)–(7), but transforming from q to r , we get the function $y(l_1, l_2, m, r)$ in r space and r frame.

(f) With the help of the PY equation (12) one can obtain the next iteration for $c(l_1, l_2, m, r)$.

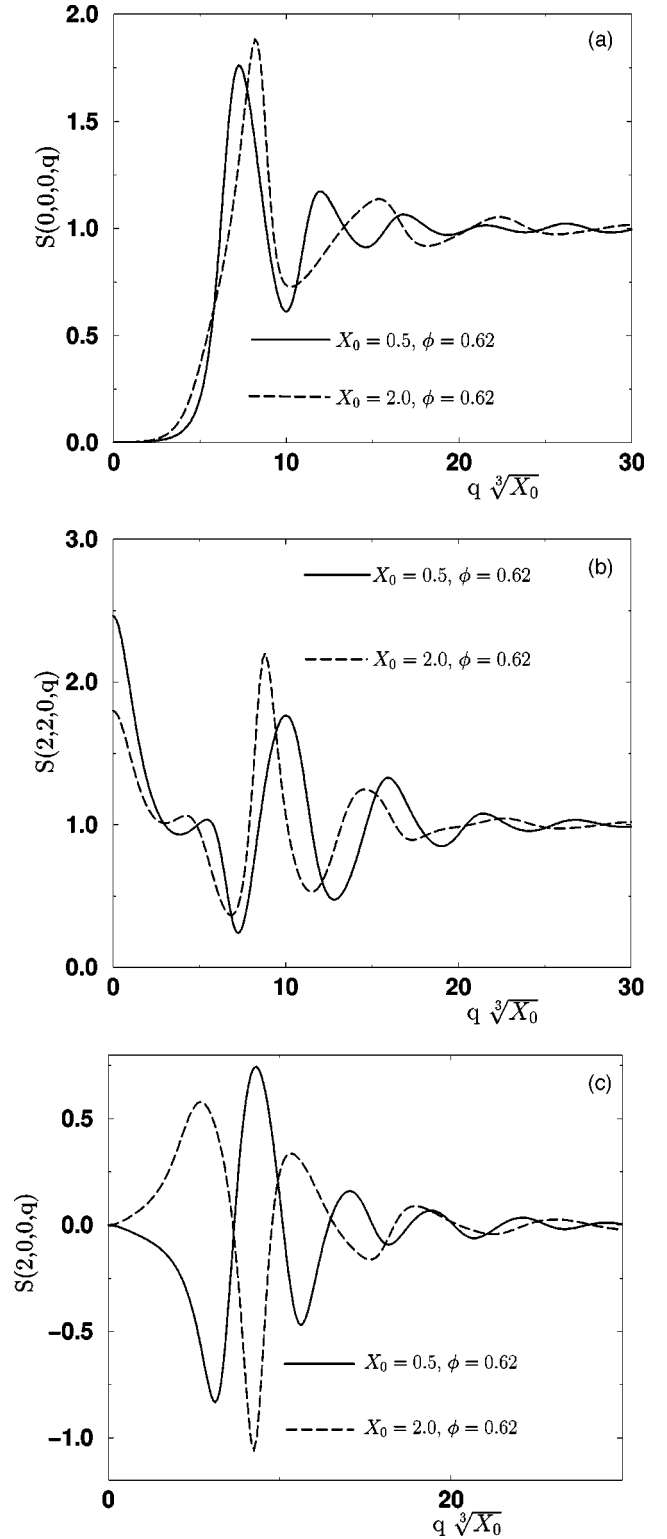


FIG. 2. In order to demonstrate the breakdown of the approximate symmetry between prolate and oblate ellipsoids ($X_0 \rightarrow 1/X_0$) we plotted for $X_0 = 2.0$ and $X_0 = 0.5$ elements of $S(l_1, l_2, m, q)$, (a) $l_1 = l_2 = m = 0$, (b) $l_1 = l_2 = 2, m = 0$, (c) $l_1 = 2, l_2 = m = 0$. The q axis was scaled by a factor of $X_0^{1/3}$.

(g) Steps (c)–(f) have to be iterated until a fix point of the equations has been reached with a given accuracy. In this way a self-consistent solution can be found.

As a test for self-consistency we choose the mean square deviation of c between two steps of iteration,

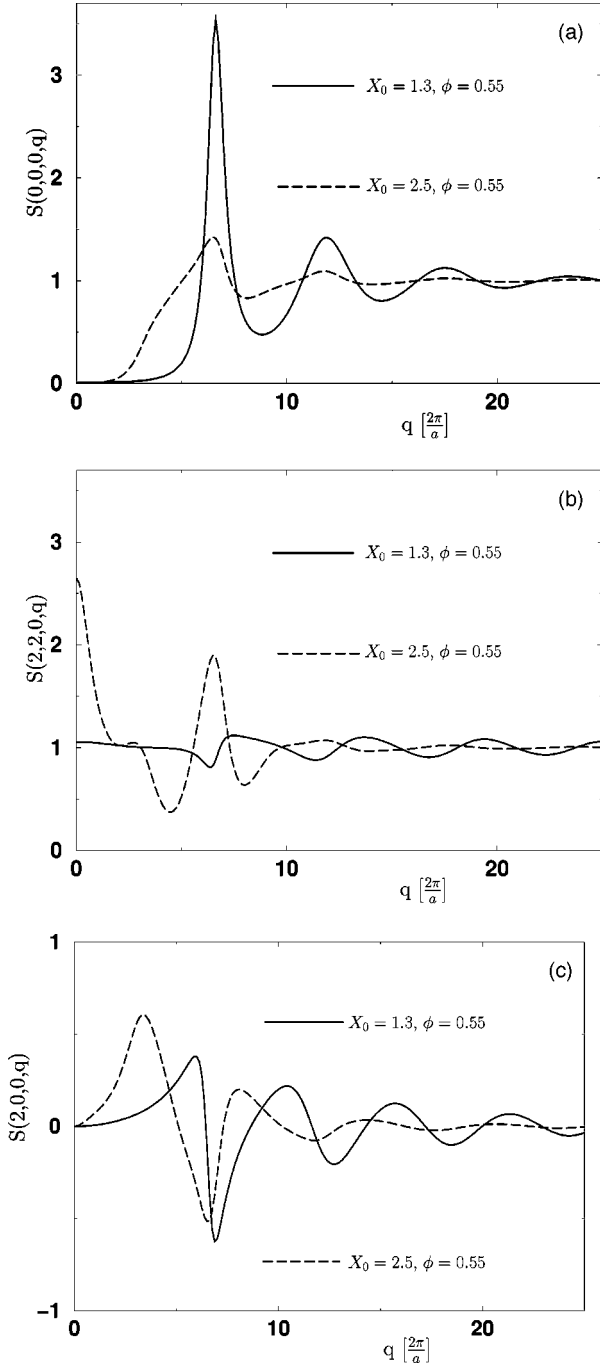


FIG. 3. The static structure factors of two systems of ellipsoids close to and far away from the nematic instability are shown by comparing the $S(l_1, l_2, m, q)$ components for $\phi = 0.55$ for $X_0 = 1.3$ (far away from the nematic instability) and for $X_0 = 2.5$ (close to the nematic instability). In part (a) the $S(0,0,0, q)$ is plotted, in part (b) $S(2,2,0, q)$, and in part (c) $S(2,0,0, q)$. Note that the $S(2,0,0, q)$ components vanish at $q = 0$ due to the symmetries.

$$\epsilon = \frac{1}{(l_{max} - 1)(m_{max} + 1)N_{max}} \times \sqrt{\sum_{l_1, l_2, m, n} [c^{(p+1)}(l_1, l_2, m, r_n) - c^{(p)}(l_1, l_2, m, r_n)]^2}, \quad (22)$$

where the summation indices were in the regions l_1, l_2

$\in \{0, 2, \dots, l_{max}\}$, $m \in \{0, 1, 2, 3, \dots, m_{max}\}$ and at the end ϵ was typically chosen to be smaller than 2×10^{-5} as a condition for convergence.

In this way one can obtain a stable self-consistent solution for the correlation functions. This has already been done for a fluid of ellipsoids in Refs. [5, 14–16] and also in Ref. [17] for a single ellipsoid in a fluid of hard spheres. In this work we have extended the calculation to a much higher density regime than has been done in previous works. In order to reach the high densities we were forced to restrict the maximum numbers for N_{max} to 400 and l_{max} and m_{max} to 4. The value of l in the rotational invariants was restricted to $l \in \{0, 2, 4, \dots, 2l_{max}\}$.

IV. RESULTS FROM THE PY EQUATION

The virial expansion of hard ellipsoids of revolution is symmetric with respect to $X_0 \rightarrow 1/X_0$ up to the second order in density. This approximate symmetry is violated for higher densities. This is shown in Fig. 2 where we have plotted three matrix elements $S(0,0,0, q)$, $S(2,2,0, q)$, and $S(2,0,0, q)$ of the static structure factor $S(l_1, l_2, m, q)$ for $\phi = 0.62$, which is related to the total correlation function $h(l_1, l_2, m, q)$ by

$$S(l_1, l_2, m, q) = \delta_{l_1, l_2} + \frac{\rho}{4\pi} h(l_1, l_2, m, q),$$

$$\underline{S}(m, q) = \underline{1} + \frac{\rho}{4\pi} \underline{h}(m, q),$$

$$\underline{S}(m, q) = \left(\underline{1} - \frac{\rho}{4\pi} \underline{c}(m, q) \right)^{-1}. \quad (23)$$

The q axis has been stretched by a factor of $\sqrt[3]{X_0}$. It can be clearly seen that a symmetry $X_0 \rightarrow 1/X_0$ is not exactly valid at such high densities.

A. Nematic instability

Close to the nematic instability the matrix element $S(2,2, m, q)$ of the static structure factor develops a divergence at $q \rightarrow 0$. This was already discussed in [5] for results based on the HNC (hypernetted chain) closure relation. In Fig. 3(b) such a precursor of a divergence is seen where for $\phi = 0.55$ two systems $X_0 = 1.3$ (far from the nematic phase) and $X_0 = 2.5$ (close to the nematic instability) are compared. For $X_0 = 1.3$ the $S(0,0,0, q)$ matrix element dominates, as can be seen from Fig. 3(a). Note also from Fig. 3 that the $S(0,0,0, q)$ components and the $S(2,2,0, q)$ seem to change their role when going from $X_0 = 1.3$ to $X_0 = 2.5$. The static structure for $X_0 = 1.3$ is dominated by the $S(0,0,0, q)$ component, while the orientational correlator $S(2,2,0, q)$ is small. This behavior is reversed when looking at $X_0 = 2.5$. Here the static structure is dominated by the orientational correlations $S(2,2,0, q)$, while the center of mass $S(0,0,0, q)$ only shows a weak structure. Due to the fact that all the nondiagonal elements of S at $q \rightarrow 0$ vanish [as can be seen in Fig. 3(c) for $S(2,0,0, q)$] only the $c(2,2, m, 0)$ component governs the nematic instability and we get as a condition for such an instability

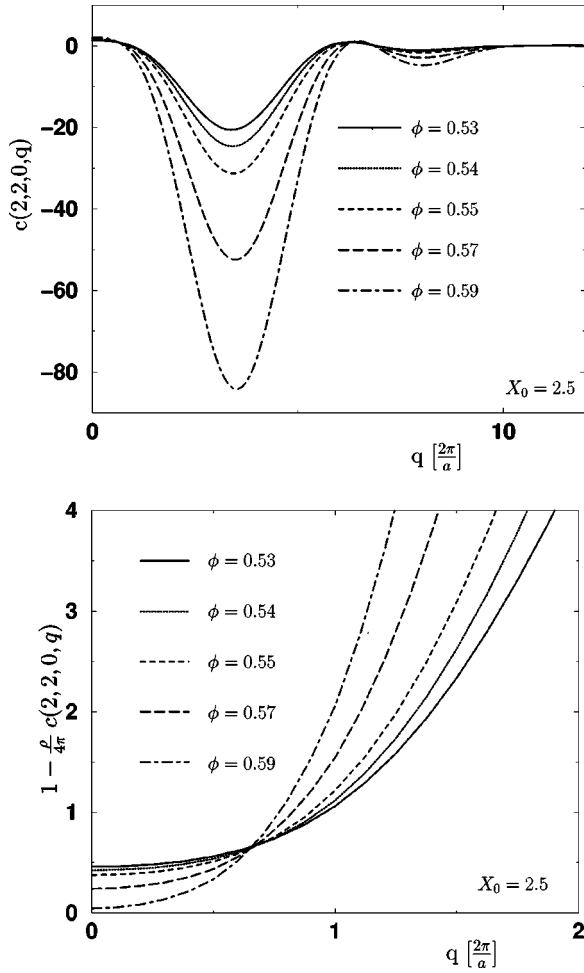


FIG. 4. In (a) $c(2,2,m,q)$ is plotted for $q \rightarrow 0$ and for different densities. The curves for $\phi=0.53,0.54,0.55$ were obtained by a solution of the PY equations, whereas the curves for $\phi=0.57,0.59$ were obtained by applying a quadratic extrapolation to higher densities to $c(2,2,0,q)$. The important part for the nematic instability is plotted in (b) where the function $1 - (\rho/4\pi)c(2,2,0,q)$ is drawn, which becomes at $q=0$ the inverse of $S(2,2,0,q=0)$.

$$\lim_{q \rightarrow 0} \left(1 - \frac{\rho}{4\pi} c(2,2,m,q) \right) \rightarrow 0. \quad (24)$$

This expression is the inverse of the Kerr constant K for nondipolar potentials:

$$K^{-1} = \lim_{q \rightarrow 0} \left(1 - \frac{\rho}{4\pi} c(2,2,m,q) \right). \quad (25)$$

A detailed analysis of the $q \rightarrow 0$ behavior therefore gives us a condition for the nematic instability such as is also discussed in a similar way in [6] where dipolar fluids in the HNC approximation have been considered. The instability is demonstrated in Fig. 4. In part (a) for $X_0=2.5$ the function $c(2,2,0,q)$ is plotted for different densities close to the nematic instability. The first three densities $\phi=0.53,0.54,0.55$ were the highest ones we could reach with the numerical solution of the PY equation, and the two higher densities $\phi=0.57,0.59$ are quadratic extrapolations. In Fig. 4(b) this is shown in greater detail where $1 - (\rho/4\pi)c(2,2,0,q)$ is plot-

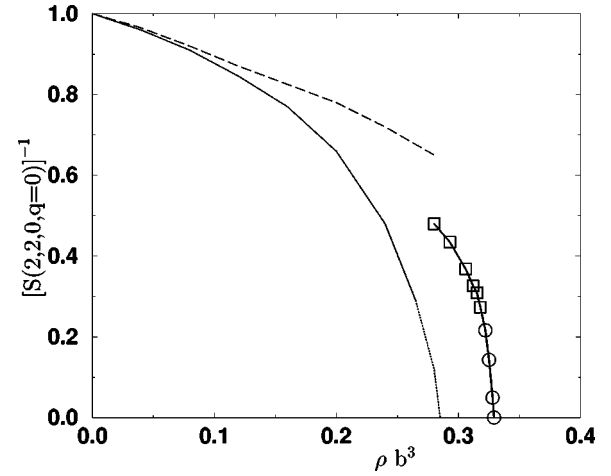


FIG. 5. For a system with an aspect ratio of $X_0=3.0$ the reduced inverse Kerr constant $[S(2,2,0,q=0)]^{-1}$ is plotted as a function of density. The thin lines are taken from Ref. [5] where the thin dashed lines are PY results, and the thin solid and thin dotted line are hypernetted chain (HNC) results and from HNC extrapolated values, respectively. The thick solid line is a result of this work obtained with the PY approximation. The points marked with squares are calculated, whereas the values at the circles were obtained using a quadratic extrapolation (see text).

ted, which becomes the inverse of $S(2,2,0,0)$ at $q=0$. For $X_0=2.5$, the critical density where $S(2,2,0,0)$ diverges is $\phi=0.593$, according to such a quadratic extrapolation. We want to mention that the convergence of the PY equations becomes extremely slow (e.g., for $\phi=0.55$ for $X_0=2.5$) close to the nematic instability. For the highest densities considered, we had to do more than 10^4 iteration steps to achieve convergence, even when starting with a well converged result for the next lower density (e.g., $\phi=0.54$). This

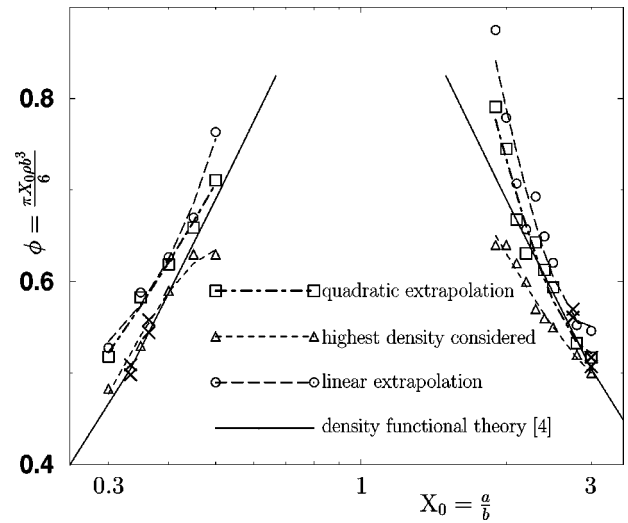


FIG. 6. Isotropic to nematic instability as it arises from a Percus-Yevick calculation. The highest densities considered are plotted with triangles. From there an extrapolation is done to determine the instability by $c(2,2,0,q \rightarrow 0) = 4\pi/\rho$. This was done with a linear (circles) and a quadratic (squares) interpolation. For comparison we plotted the IN transition, which arises from density-functional theory [4]. Also the results from Ref. [3] are plotted with black crosses.

is probably the reason why the nematic instability has not been discovered in previous works [5,7]. For comparison we have plotted in Fig. 5 our result for $X_0=3.0$ together with the result of Ref. [5]. We do not only find a nematic instability with the PY approximation but also get a density where this instability occurs, which is much closer to the Monte Carlo simulation results of [3] ($\rho_c \approx 0.32$) than the result from the hypernetted chain approximation of Ref. [5].

B. Equilibrium phase diagram

Using the above condition [Eq. (24)] we get the phase diagram for the hard ellipsoids as it arises from the PY approximation as shown in Fig. 6. For all densities considered there results a clear indication for a nematic instability. This phase boundary still depends on the way the extrapolation to higher densities is done (here linear or quadratic), but is in good agreement with other works. For example, the density-functional theory of Groh and Dietrich [4] is in a reasonable good agreement with our results. However, due to their approximation the X_0 to $1/X_0$ symmetry is exact, which is however clearly broken in the PY result. Also the results of Frenkel *et al.* [3] are along the same lines. It also seems that density-functional theory shows a better agreement with PY theory for prolate ellipsoids than for oblate ones.

V. CONCLUSION

Oriental degrees of freedom in molecular systems can drive a phase transition into an orientationally ordered nematic liquid crystal phase. In principle, integral equations have the ability to describe a precursor phenomenon of such an orientational transition. Until now this is well known for, e.g., hypernetted chain (HNC) theory. In this work we demonstrate that Percus-Yevick theory also shows a clear precursor of the nematic phase. We therefore were able to calculate the equilibrium phase diagram of hard ellipsoids of revolution. The obtained phase diagram is in good agreement with density-functional theory [4] and Monte Carlo simulations [3].

ACKNOWLEDGMENTS

M.L. thanks Mike Allen for making his results of computer simulations available, which made us quite confident about the quality of the Percus-Yevick results. We are further grateful to R. Schilling for valuable and helpful discussions and acknowledge financial support from the Deutsche Forschungsgemeinschaft through SFB 262.

-
- [1] J. P. Hansen and I. R. McDonald, *Theory of Simple Liquids* (Academic, London, 1976).
- [2] L. Onsager, Ann. (N.Y.) Acad. Sci. **51**, 624 (1949).
- [3] D. Frenkel, B. M. Mulder, and J. P. McTague, Phys. Rev. Lett. **52**, 287 (1984).
- [4] B. Groh and S. Dietrich, Phys. Rev. E **55**, 2892 (1997).
- [5] A. Perera, P. G. Kusalik, and G. N. Patey, J. Chem. Phys. **87**, 1295 (1987).
- [6] S. Klapp and F. Forstmann, J. Chem. Phys. **106**, 9742 (1997).
- [7] A. Chamoux and A. Perera, J. Chem. Phys. **104**, 1493 (1996).
- [8] C. G. Gray and K. E. Gubbins, *Theory of Molecular Fluids* (Clarendon, Oxford, 1984).
- [9] P. T. Cummings, J. Ram, R. Barker, C. G. Gray, and M. S. Wertheim, Mol. Phys. **48**, 1177 (1983).
- [10] C. G. Gray and K. E. Gubbins, *Theory of Molecular Fluids* (Ref. [8]), Appendix A, p. 506.
- [11] B. J. Berne and P. Pechukas, J. Chem. Phys. **56**, 4213 (1972).
- [12] M. P. Allen, C. P. Mason, E. de Miguel, and J. Stelzer, Phys. Rev. E **52**, R25 (1995).
- [13] R. Schilling and T. Scheidsteger, Phys. Rev. E **56**, 2932 (1997).
- [14] R. Pospisil, A. Malijevsky, and W. R. Smith, Mol. Phys. **79**, 1011 (1993).
- [15] J. Ram and Y. Singh, Phys. Rev. A **44**, 3718 (1991).
- [16] J. Ram, R. C. Singh, and Y. Singh, Phys. Rev. E **49**, 5117 (1994).
- [17] T. Franosch and A. P. Singh, J. Chem. Phys. **107**, 5524 (1997).